Experimental and Numerical Study on the Flow Ripple of Circular-arc Gear Pumps Considering the Center Distance Deviation

Xiaoling Wei (weixiaolng800@163.com)
PLA Rocket Force University of Engineering Department of Missile Engineering https://orcid.org/0000-0003-1729-4300

Yongbao Feng
PLA Rocket Force University of Engineering Department of Missile Engineering

Zhenxin He
PLA Rocket Force University of Engineering Department of Missile Engineering

Ke Liu
PLA Rocket Force University of Engineering Department of Missile Engineering

Original Article

Keywords: Circular-arc Gear Pump, Center Distance, Flow Ripple, Pressure Ripple

Posted Date: August 31st, 2021

DOI: https://doi.org/10.21203/rs.3.rs-841282/v1

Experimental and Numerical Study on the Flow Ripple of Circular-arc Gear Pumps Considering the Center Distance Deviation

Xiaoliing Wei [1,*], Yongbao Feng [1], Zhenxin He [1] and Ke Liu [1]

1. PLA Rocket Force University of Engineering, 710025 Xi'an, China;
*Correspondence: weixiaoling800@163.com

Abstract: Novel circular-arc gear pumps effectively solve the problems of oil trapping and flow pulsation experienced with traditional gear pumps. However, the center distance deviation associated with assembly and installation during gear pump processing has an important influence on the outlet pressure pulsation characteristics of circular-arc gear pumps. First, the circular-arc tooth profile equation, conjugate curve equation and meshing line equation were derived to design the circular-arc gear meshing and center distance deviation functions. Second, the circular-arc gear tooth profile was accurately obtained. Then, a pressure pulsation characteristic simulation model for the novel circular-arc gear pumps considering the center distance deviation was established. The results show that with the increase of center distance deviation, the outlet flow rate of the arc gear pump increases first and then decreases greatly. Moreover, the center distance deviation has little effect on the independent tooth cavity pressure. Finally, the proposed fluid dynamic model is used to simulate a commercial circular-arc gear pump, which was tested within this research for modeling validation purposes. The comparisons highlight the validity of the proposed simulation approach.

Keywords: Circular-arc Gear Pump, Center Distance, Flow Ripple, Pressure Ripple

1. Introduction

Among the existing positive displacement pumps, external gear pumps are mainly used in systems such as fuel injection systems, automotive lubrication and transmission systems, and high-pressure cleaning and fluid delivery systems [1]. The main advantages of this type of pump are that the manufacturing cost is low, the packaging is compact, it can operate at high pressures, it is suitable for fluids in the high-viscosity range, and it has high resistance to fluid variations and cavitation. However, the traditional involute external gear pump is limited by uneven outlet flows due to an oil trapping phenomenon, which causes the pump to produce noise and vibrations [2].

Researchers have begun to study unconventional tooth profiles, including arc gears, to further reduce the pulsation of the outlet flow. Morselli [3] first described an arc gear pump in a patent, and Chen and Yang [4] published the first research results obtained with an arc tooth profile in an external gear pump. Zhou Yang et al. [5] discussed the tooth profile design in detail and combined involute and arc tooth profiles. Manring, Kasaragadda [6], Huang, Lian [7], and others proposed a basic method to link spur gear tooth profile parameters with motion flow pulsation. Vacca et al. [8] applied this method to circular arc gear pumps and theoretically analyzed determined that the outlet flow pulsation for circular arc gear pumps was zero; however, experimental research results indicated that circular arc gear pumps yielded very small pressure and flow pulsations. R. Massimo [9] reviewed different flow simulation methods to simulate the flow of gear drives and external gear pumps before 2017. For the lumped parameter model, the flow simulation of different pumps based on the control volume was analyzed, the control equation was given, and the latest research results considering the effect of the interaction of fluid and mechanical components on leakage were introduced. Dipen R et al. [10] simulated the internal fluid motion state of an involute external gear pump through FLUENT software, and compared them through experiments, and obtained the good results.

The center distance deviation in the assembly of the circular-arc gear pump changes the contact position and contact area of the gear tooth surface, thus affecting outlet pressure pulsation and resulting in vibration and noise. Therefore, it is necessary to study how the center distance deviation affects the dynamic characteristics of the circular-arc gear pump, which will help to guide the gear design and machining of the circular-arc gear pump, so as to lay a foundation for giving full play to its performance advantages. In this paper, according to the principle of spatial meshing, we derived the end face tooth profile equation, conjugate tooth profile equation and meshing line equation for circular-arc gears. On this basis, the effects of the tooth profile and center distance deviation on flow pulsation and pressure pulsation are studied for a circular-arc gear pump, which provided the theoretical guidance for the circular-arc gear design.

2. The Center distance deviation and the Meshing Position

Figure 1 shows the change in the meshing position with and without center distance deviation when the arc gears are meshed. The driving gear produces an offset positionΔL, and the offset position of the driven gear is zero. **Figure 1**(**a**) shows that the theoretical center distance is L, and the driving gear and the driven gear mesh at point M_0 when there is no center distance deviation. The driving gear and the driven gear mesh at point M_1 when there is a center distance deviation ΔL (which is positive here). **Figure 1**(**b**) is an enlarged view of the meshing position.

Because the driving and driven gears may have offset positions in reality and the operation process, CNC machining technology and installation process are characterized by inherent errors, the center distance deviations in this article are 0, 0.01 mm, and 0.02 mm.

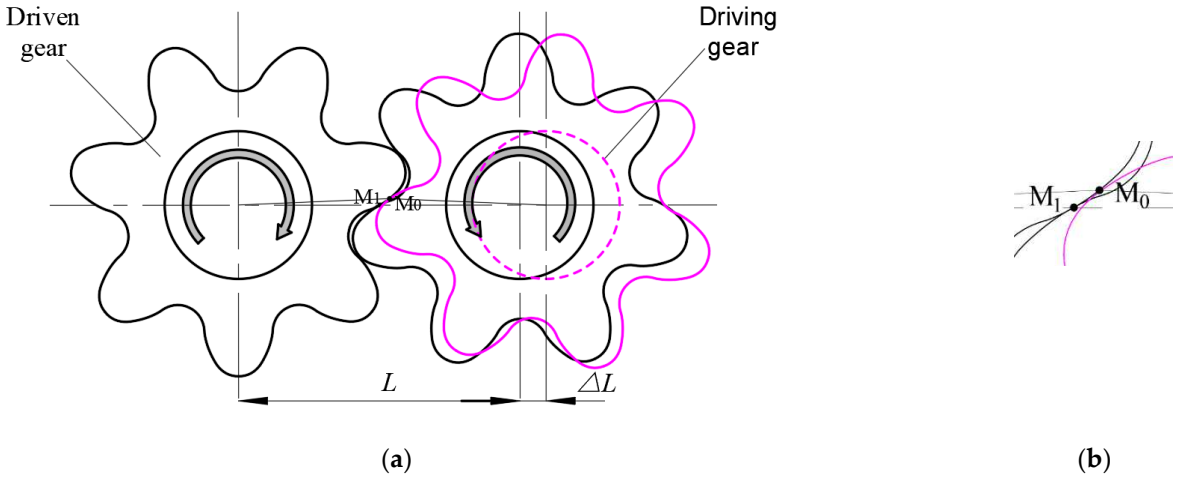

(**a**) (**b**)

Figure 1. Schematic diagram of basic tooth profile for the meshing of arc gears with and without center distance deviation: (**a**) the driving gear and the driven gear mesh at point M_0 when there is no center distance deviation. The driving gear and the driven gear mesh at point M_1 when there is a center distance deviation; (**b**) is an enlarged view of the meshing position.

3. Geometric Modeling

3.1. Arc Tooth Profile Equation

The arc gear adopts a tooth profile based on an arc curve-involute-arc curve design; the top and root of the gear have an arc curve design, and the side of the gear has an involute design to form a set of conjugate curves.

Because the tooth profile of the involute gear is symmetrical, we only assess half (N/2) of the tooth profile. The curve ABCD from the highest point A on the gear tooth to the lowest point D in the adjacent tooth valley is selected as the research focus. This curve segment is located within the angle$\angle AO_1D$, where$\angle AO_1D = \pi/N$ and N is the number of teeth. Taking the base circle center point O_1 as the coordinate origin, the line connecting any point M on the base circle, and circle center point O_1 as the horizontal axis, we establish a plane rectangular coordinate system xOy, as shown in **Figure 2**(**a**). This part of the curve is composed of the involute curve BC and two arc curves AB and CD, where the two arc curves are tangential to the involute curve at points B and C. Due to the symmetry of the tooth profile [5], the arc curve AB is perpendicular to the straight line O_1A at point A, and the arc curve CD is perpendicular to the straight line CD at point D. We obtain the tangents to the base circle separately through points B and C and the tangents at points B' and C'. Since the two arc curves are tangential to the involute curve at points B and C, the intersection point A' of the straight line BB' and the straight line O_1A is the center of the arc curve AB, and the intersection point D' of the straight line CC' and the straight line O_1D is the center of the arc curve CD.

Assuming that the radius of the base circle is r and the angles $\angle MO_1A$, $\angle MO_1C'$ and$\angle MO_1B'$ are given by θ_A, θ_C and θ_B, respectively, the involute tooth profile portion of the arc g$\angle$ear pump can be represented by the above 4 parameters. These four parameters are used to establish the involute equation, the coordinates of the centers of A_1' and D_1', and the coordinates of the radii r_1 and r_2 to determine the expression of the addendum radius r_a and the root radius r_f. The current point Q is established on the involute line, and the tangent to the base circle passing through Q is the involute generation line. The tangent point is then Q', and the angle $\angle Q'O_1M$ is α.

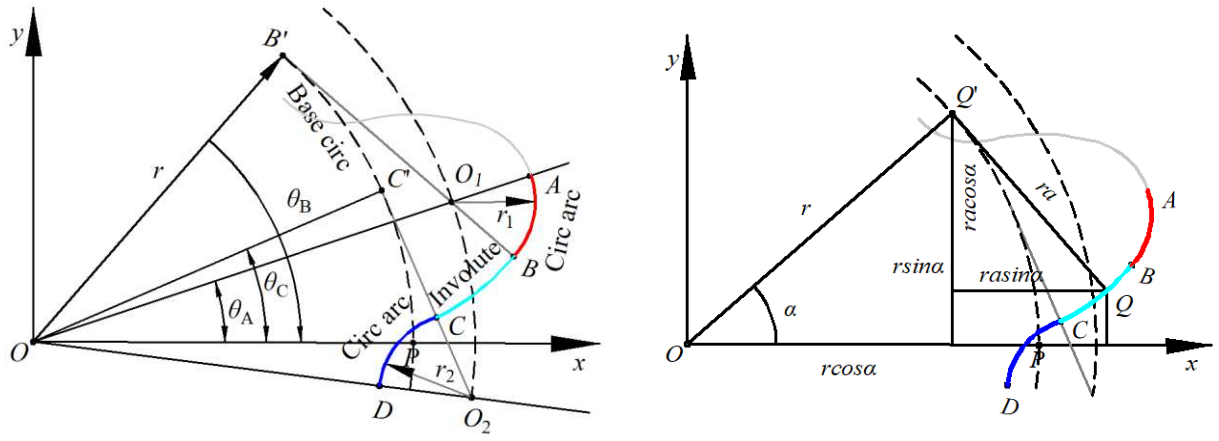

(**a**) (**b**)

Figure 2. Gear tooth profile: (**a**) the curve is composed of the involute curve BC and two arc curves AB and CD, where the two arc curves are tangential to the involute curve at points B and C; (**b**) Description the relationship of the AB section of the arc curve, the involute BC section, and the CD section of the arc curve.

From **Figure 2**(**b**), the involute BC section equation is obtained:

$$\left.\begin{aligned} x_{12} &= r\cos\alpha + r\alpha\sin\alpha \\ y_{12} &= r\sin\alpha - r\alpha\cos\alpha \end{aligned}\right\}. \tag{1}$$

The equation of the AB section of the arc curve is:

$$\left.\begin{aligned} x_{11} &= \frac{r\cdot\cos\theta_A}{\cos(\theta_A-\theta_C)} + r_1\sin\varphi_1 \\ y_{11} &= \frac{r\cdot\sin\theta_A}{\cos(\theta_A-\theta_C)} + r_1\cos\varphi_1 \end{aligned}\right\}, \tag{2}$$

where φ_1 is a parameter related to the arc angle of the AB segment. The CD segment equation of the arc curve is:

$$\left.\begin{aligned} x_{13} &= \frac{r\cdot\cos\left(\theta_A-\frac{\pi}{N}\right)}{\cos\left(\theta_B-\left(\theta_A-\frac{\pi}{N}\right)\right)} + r_2\sin\varphi_2 \\ y_{13} &= \frac{r\cdot\sin\left(\theta_A-\frac{\pi}{N}\right)}{\cos\left(\theta_B-\left(\theta_A-\frac{\pi}{N}\right)\right)} + r_2\cos\varphi_2 \end{aligned}\right\}, \tag{3}$$

where φ_2 is a parameter of the arc angle of the CD segment. Then, the addendum radius r_a is:

$$r_a = r\cdot\sec\left(\theta_B-\left(\theta_A-\frac{\pi}{N}\right)\right) - r\cdot\theta_B \tag{4}$$

The root radius r_f is

$$r_f = r\cdot\sec(\theta_c-\theta_A) - r\cdot\tan(\theta_c-\theta_A) + r\cdot\theta_c \tag{5}$$

Since the tooth profile is formed by the smooth connection between the arcs A_1B_1 and C_1D_1 and the involute curve B_1C_1 and the connecting points of the arc and the involute are B_1 and C_1, the points B_1 and C_1 are both on the arc and the involute curve; thus, the three curves are connected. Therefore,

$$\left.\begin{aligned} \varphi_{1B} &= -\arctan\theta_B \\ \varphi_{2C} &= -\arctan\theta_C \end{aligned}\right\}, \tag{6}$$

where

$$\left.\begin{aligned}\theta_B &= \tan\alpha + \frac{\pi}{2N}\\ \theta_C &= \tan\alpha - \frac{\pi}{2N}\end{aligned}\right\} \tag{7}$$

The above formula sets indicate that the tooth profile of the end face of the arc gear pump is influenced by the base radius r; the opening angles θ_A, θ_C and θ_B; and the number of teeth.

3. 2. Conjugate Arc Tooth Profile Equation

After determining the curve equation for a section of the driving gear, the conjugate curve equation of the driven gear can be obtained by the principle of conjugate gear meshing [9]. The specific solution process is as follows.

As shown in **Figure 2**(**a**), points O_1 and O_2 are the centers of the gears, and point P is the pitch point of the gear pair. The pitch circle radius is r_1, and the center distance is a (O_1O_2=2r_1). We take O_1 as the origin of the coordinate system S_1 (O_1-x_1, y_1), which is fixed, connected to gear 1 and rotates with gear 1. O_2 is the origin of the coordinate system S_2 (O_2-x_2, y_2), which is fixed, connected to gear 2 and spins with gear 2. We use point P as the origin to fix the coordinate system S_P (P-x, y) on the meshed two-gear transmission plane. At the starting position, the coordinate axes y_1 and y_2 coincide with y, and the coordinate axes x_1 and x_2 are parallel to x.

The known tooth profile ABCD is fixed and connected with the coordinate system S_1 (O_1-x_1, y_1). Gear 1 and the tooth profile ABCD rotate counterclockwise together. The rotation angle of gear 1 is positive in the counterclockwise direction. We can assume that the angle between the tangent at a point N (x_1, y_1) on the tooth profile ABCD and the axis x_1 is γ. The normal line intersects the pitch circle of gear 1 at point N', and the angle between the straight line O_1 N' and the tangent at point N is θ. Each point on the tooth profile ABCD is a contact point. By transforming coordinates of arc AB, the involute curve BC, and the arc CD into coordinate system S_2 (O_2-x_2, y_2), which is fixed and connected to gear 2, we can obtain the conjugate gear tooth profile equation:

$$\begin{bmatrix}x_2\\ y_2\\ t_2\end{bmatrix} = \begin{bmatrix}\cos 2\varphi & -\sin 2\varphi & 2r_1\sin\varphi\\ \sin 2\varphi & \cos 2\varphi & -2r_1\cos\varphi\\ 0 & 0 & 1\end{bmatrix}\begin{bmatrix}x_1\\ y_1\\ t_1\end{bmatrix}, \tag{8}$$

where t is equal to 1.

3. 3. Meshing Line Equation

The trajectory of the contact point in the fixed coordinate system S_P (P-x, y) is the meshing line. Based on coordinate transformation, the meshing line equation can be obtained:

$$\begin{bmatrix}x\\ y\\ t\end{bmatrix} = \begin{bmatrix}\cos\varphi & -\sin\varphi & 0\\ \sin\varphi & \cos\varphi & -r_1\\ 0 & 0 & 1\end{bmatrix}\begin{bmatrix}x_1\\ y_1\\ t_1\end{bmatrix}, \tag{9}$$

where

$$\left.\begin{aligned}\cos\theta &= \frac{x_1\cos\gamma + y_1\sin\gamma}{r_1}\\ \varphi &= \frac{\pi}{2} - (\gamma + \theta)\\ \tan\gamma &= \frac{dy_1}{dx_1}\\ r_1 &= \frac{r_a + r_f}{2}\end{aligned}\right\} \tag{10}$$

By determining the coordinates of a point on the tooth profile ABCD and calculating the angle γ between the tangent of this point and axis x_1 based on (10), the angle of rotation when the point becomes the contact point can be calculated. To ensure continuous transmission for the gear pump, this paper focuses on half of the pitch angle 2π/N:

$$\beta \geq \frac{\pi}{N} \tag{11}$$

4 Fluid Dynamic Model

4.1 Governing Equation

Within each tooth space, the following pressure build-up equation is solved for the pressure dynamics [11]:

$$\frac{dp}{dt} = \frac{K}{V}[Q - \dot{V}] \tag{12}$$

where K is the bulk modulus, V is the instantaneous tooth space volume, $\dot{V}$ is the change rate of tooth space volume, while Q is the flow in the tooth space. Each tooth space solves its own pressure build-up equation, i.e. Eq. (12).

The turbulent orifice connections of each tooth space are considered in this paper, similarly to the approach of [12]. For this turbulent orifice connection, the flowrate is given by:

$$Q = C_q \cdot A \cdot \sqrt{\frac{2|\Delta p|}{\rho}} \tag{13}$$

Where the C_q is the discharge coefficient, A is the orifice opening area, Δp is the pressure difference between displacement chambers at both ends, and ρ is the density taken at the average pressure between displacement chambers at both ends. To take the influence of the Reynolds number on the discharge into account, the discharge coefficient is modeled as [13].

$$C_q = C_{qmax} \cdot tanh\left(\frac{2\lambda}{\lambda_{crit}}\right) \tag{14}$$

where the C_{qmax} is the user defined empirical maximum flow coefficient, and the typical value used is 0.7. The hyperbolic tangent function is generally used to fit the case of low Reynolds number. The k is the predictive quantity of Reynolds number, which is estimated as:

$$\lambda = \frac{D_h \cdot u}{v} = \frac{D_h}{v}\sqrt{\frac{2\Delta p}{\rho}} \tag{15}$$

The typical value of the critical Reynolds number λ_{crit} for orifice plate is 1000 [13]. When the Reynolds number is low, the hyperbolic tangent function makes the flow rate change linearly with the pressure difference and returns to the state of flow field. The D_h is the hydraulic diameter of orifice opening, and the velocity at orifice is estimated as

$$u = \sqrt{\frac{2\Delta p}{\rho}} \tag{16}$$

4.2 Implementation

The overall numerical model of an arc gear pump is established, as shown in **Figure 3**. The 1D model of the arc gear pump is automatically generated so that the arc tooth profile can be accurately obtained. The center distance deviation was considered in advance.

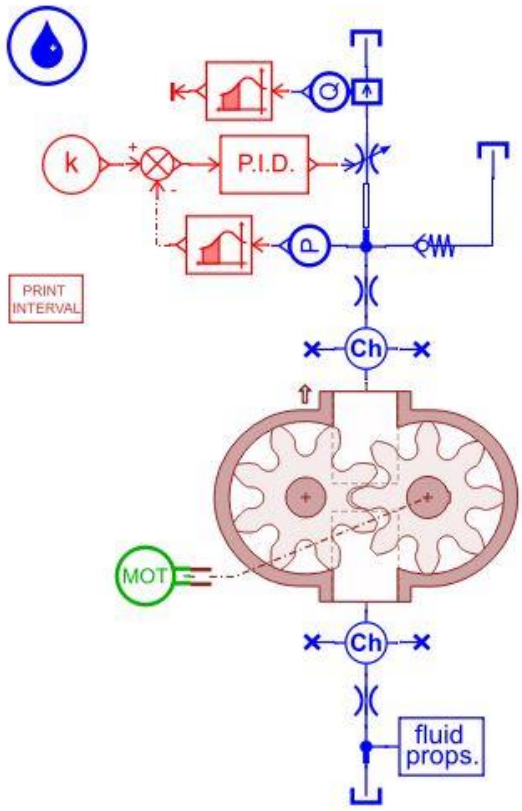

Figure 3. The overall numerical model of an arc gear pump.

We established a three-dimensional model of the arc gear pump and then created a 1D model of the arc gear pump according to the CAD import function. It should be noted that the center of the coordinate system of the arc gear pump must be located at the 1D center of the driving gear, and the arc gear rotates counterclockwise. According to the 1D model of the arc gear pump, the initial associated parameters can be obtained, as shown in **Table 1**. The initial parameters of the overall simulation model were set as shown in **Table 2**.

Table 1. 1D model initial correlation parameters of the arc gear pump.

Parameters	Values
Center distance	39.17 mm, 39.18 mm, and 39.19 mm
Initial pressure	0 bars
Number of teeth of gear	7
Gear thickness	31 mm
Teeth clearance	0.1 mm
Radial clearance	0.001 mm
Length gap tooth	0.3 mm
Width gap tooth	0.4 mm
Height left gap tooth	0.001 mm
Height right gap tooth	0.001 mm[1]

[1] Data are from the 1D model of the arc gear pump.

Table 2. Initial parameter values for the arc gear pump simulation.

Parameters	Values
Fluid property file	ISO VG 46 oil - Mobil DTE 25
Temperature	30℃

Shaft speed	1480 rev/min[2]

[2]Data are from the initial parameters of the overall simulation model in AMESim.

When the simulation model of the arc gear pump was established, each tooth volume during the meshing of the driving gear and the driven gear was determined, as shown in **Figure 4.** The driving gear (right) drives the driven gear (left) to rotate counterclockwise and perform oil suction and discharge functions for the arc gear pump. The volumes enclosed by the dotted lines are the volumes of the fourth tooth of the driving gear and the driven gear, denoted as Dr#4 and Dn#4. Based on counterclockwise rotation, all the intertooth volumes of the pump are marked. Notably, Dr represents the driving gear, Dn represents the driven gear, and *i* (*i*=1, 2…7) represents the *i*-th intertooth volume.

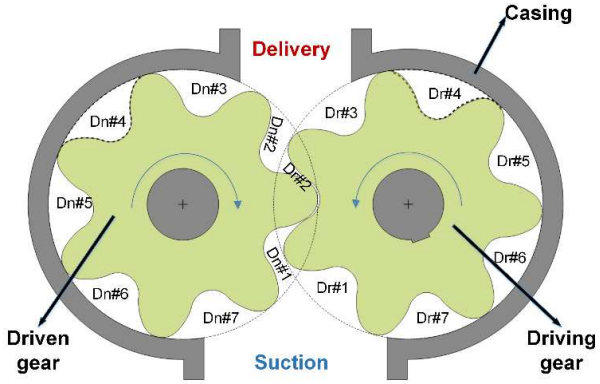

Figure 4. Working principle diagram of the arc gear pump. The driving gear is on the right, and the driven gear is on the left. The driving gear (right) drives the driven gear (left) to rotate counterclockwise.

5. Model Results and Validations

Pressure ripple and flow ripple have been carried out in full flow condition and in zero flow condition with outlet pressures of 0, 20, and 80 bar and constant rotational speed of 600 rpm and 1480 rpm in different Center Distances.

5.1. Simulation results on the reference pump and discussion

5.1.1Effect of Different Center Distances on Flow Rates

Figure 5 shows the influence of the center distance deviation on the pulsation of the pump outlet flow. Under the light load condition (600rpm, 20bar), with the increase of center distance deviation, the outlet flow rate of the arc gear pump increases first and then decreases greatly. When the center distance deviation is within 0.01mm, the outlet flow rate of the arc gear pump increases gradually and has good dynamic characteristics. As the center distance deviation increases to 0.02mm, the outlet flow rate of the arc gear pump decreases greatly, and the dynamic characteristics of this pump become worse. Under the medium load condition (1480rpm, 80bar), with the increase of center distance deviation, the outlet flow rate of arc gear pump shows the same characteristics as the light load condition. In conclusion, the arc gear pump is more sensitive to the center distance deviation. When the center distance deviation is controlled within a certain range, the arc gear pump has better dynamic characteristics. Therefore, in order to give full play to the good transmission performance of the arc gear pump and prevent excessive dynamic impact due to the center distance deviation, the dynamic response caused by the center distance deviation can be adjusted by optimizing the machining accuracy and assembly accuracy of the arc gear.

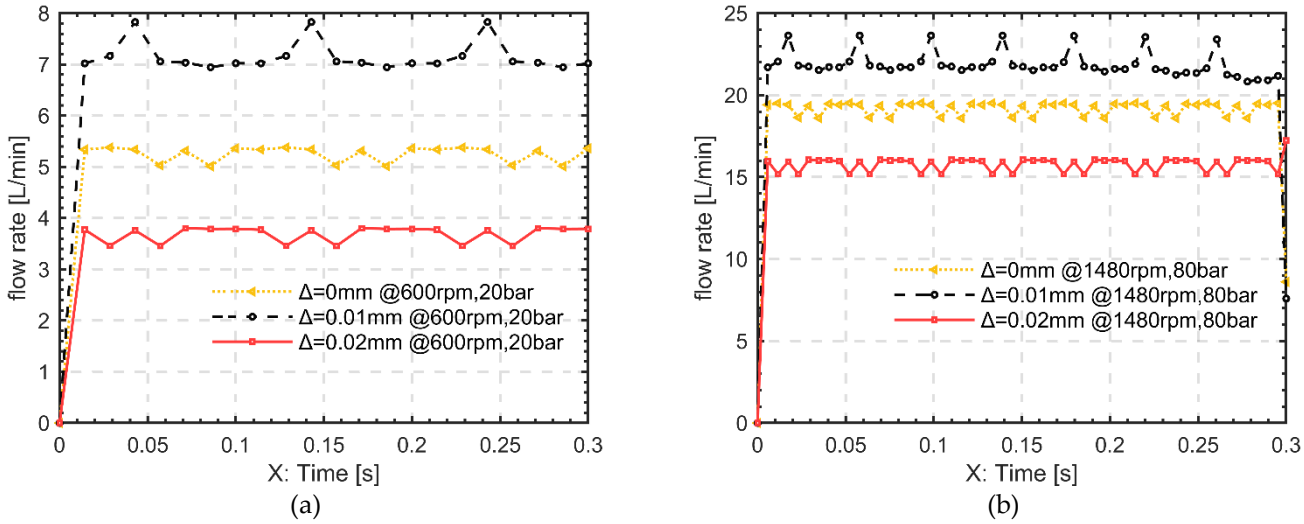

Figure 5. The influence of the center distance deviation on the pulsation of the pump outlet flow: (a) the light load condition is 600rpm & 20bar; (b) the medium load condition is 1480rpm & 80bar.

5.1.2. Effect of Different Center Distances on Pressure

The pump speed was set to 1480 r/min, and the pressure changes in each tooth volume for the driving and driven gears were observed with center distance deviation, shown in **Figure 6**. When the arc gear pump starts to run, the first tooth volume of the driving gear is completely connected to the pump inlet, and the pressure associated with the tooth volume is the same as the inlet pressure. Approximately 90% of the first tooth volume of the driven gear is connected to the pump outlet. Thus, at initial moment, pressure in the volume is lower than the outlet pressure. The pressure in the tooth volume then gradually decreases with the operation of the pump. As the center distance deviation gradually increases, the pressure in the first volume of the driving gear does not change, and the pressure in the first volume of the driven gear has micro oscillations. When the arc gear pump continue to run, 95% of the second tooth cavity of the driving gear and driven gear are connected to the pump outlet. At this time, the pressure in the tooth cavity is equal to the pump outlet pressure. As the center distance deviation gradually increases, the pressure in the second cavity of the driving and driven gears has no change. The third tooth cavity and of the driving gear is completely connected to the pump outlet. At this time, the pressure in the tooth cavity is the same as the pump outlet pressure. The third tooth cavity of the driven gear is an independent tooth cavity that is not connected to any port of the pump. The pressure in the tooth cavity gradually reaches the outlet pressure. As the center distance deviation gradually increases, the pressure in the third cavity of the driving gear has no change. The 4th tooth cavity and of the driving gear and driven gear are the independent tooth cavities that are not connected to any port of the pump. As the center distance deviation gradually increases, the pressure in the third cavity of the driving gear has no change. The 7th tooth cavity of the driving and driven gears are connected to the pump inlet. The pressure on the driving gear smoothly decreases.

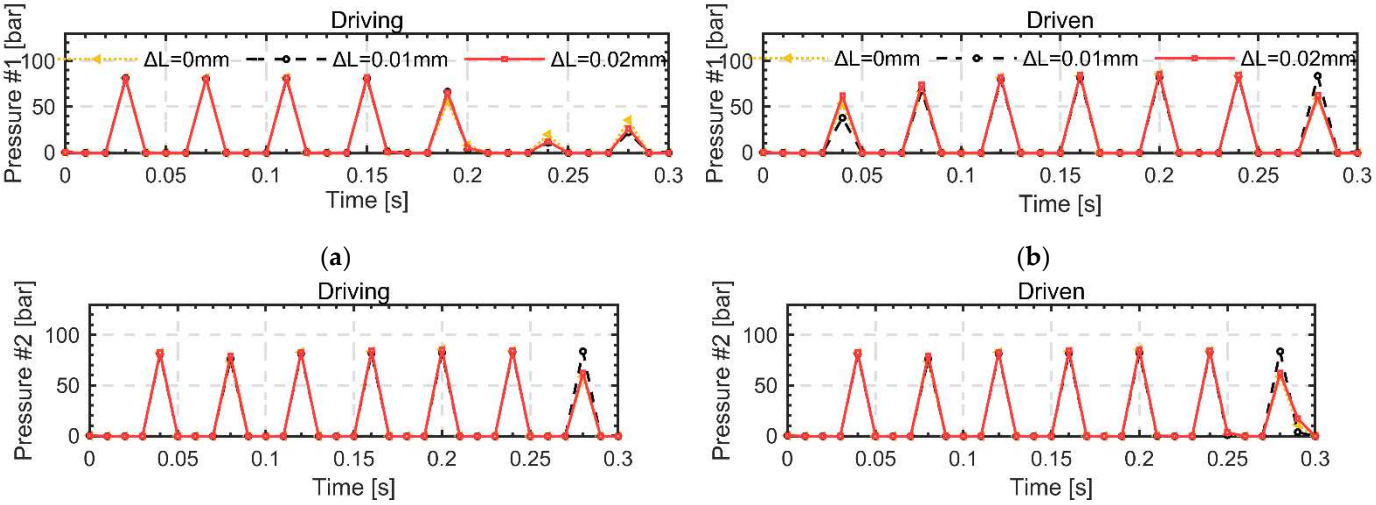

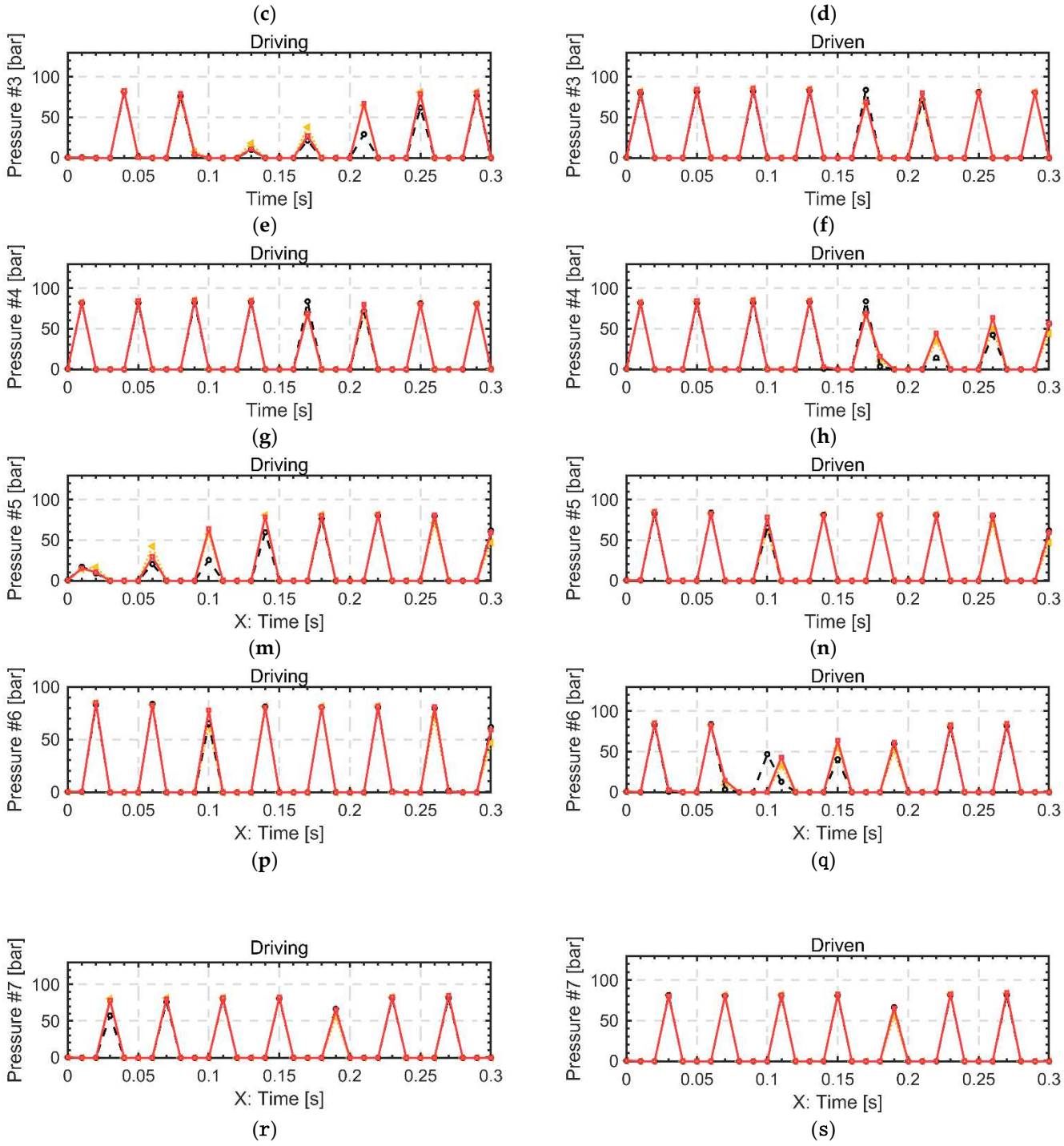

Figure 6. The effect of center distance deviations on pressure for each tooth cavity at 1480rpm and 80bar.

5.2. Experimental measurement and validation

Experiments were conducted on a commercial circular-arc gear pump produced by Settima. The ISO schematic of the experimental setup is shown in **Figure 7**. The model under test was a 7-tooth gear pump of 32 cm^3/rev displacement**.** The tests were performed at the Shandong Shijing Machinery Co.Ltd，shown in **Figure 8**. The information about the sensors used in the setup is presented in the **Table 3**. The fluid used during the test is the ISO VG 46 hydraulic oil.

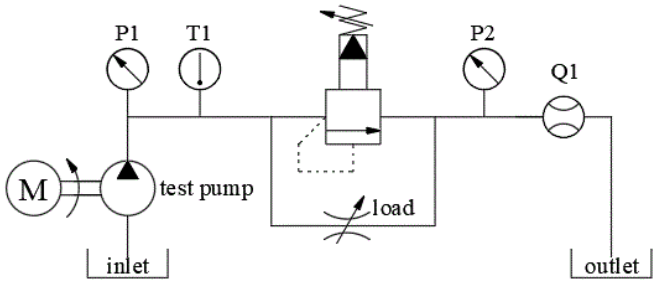

Figure 7. ISO schematic of the experimental setup.

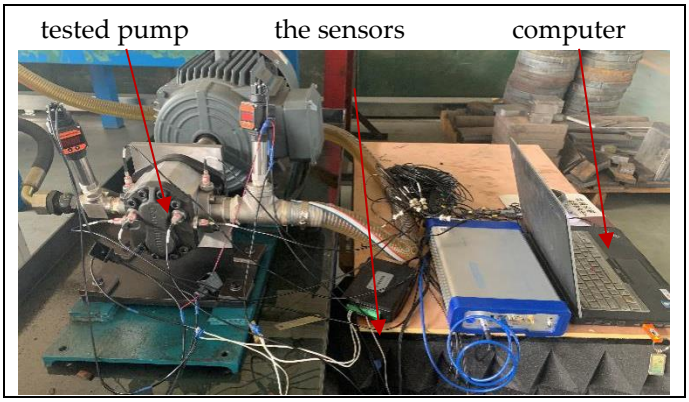

Figure 8. The experiment setup.

Table 3. Senor data of the experimental setup.

Name	Senor type	Range	Precision
P1	MIK-P300-30MPa-V1-B1-C1-J1P1	0~300bar	0.5%
P2	MIK-P300-30MPa-V1-B1-C1-J1P1	0~300bar	0.5%
Q1	BELZ-0	1~6m³/h	0.5%

Tests were performed for different shaft speeds (600 rpm, 1000 rpm, and 1480 rpm) with various pressure differentials up to 80 bar. The pump parameters were also measured to reproduce the gear profile in simulation. The comparisons between outlet pressure oscillations and outlet flow oscillations are reported in the following part of this section.

Two representative cases of the outlet pressure oscillations and outlet flow oscillations comparisons are shown in **Figure 9** and **10**. **Figure 9** shows a high-speed and high-pressure case, in which the outlet pressure and flow behavior are exhibited: for different center distance deviations, the outlet pressure oscillations are match the experiment, however, the outlet flow rate have great oscillations, and the flow behavior is same to the case of center distance deviation 0 to 0.01mm. While **Figure 10** shows a low-speed and low-pressure case, in which the outlet pressure and flow behavior are exhibited: for different center distance deviations, the outlet pressure of simulation have not any change, but the outlet pressure of experiment has oscillations, as well as the outlet flow result of experiment is greater than the simulation.

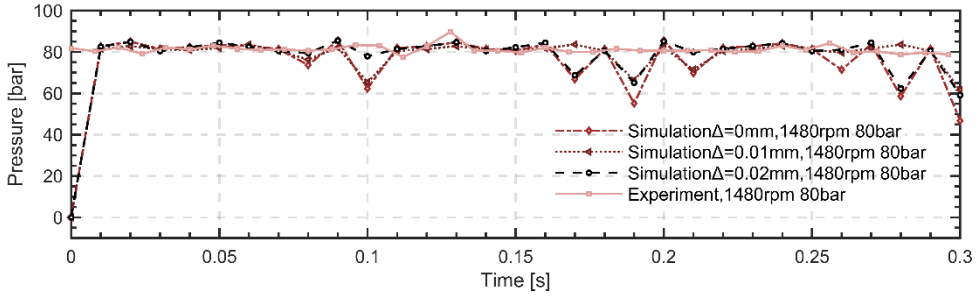

(**a**)

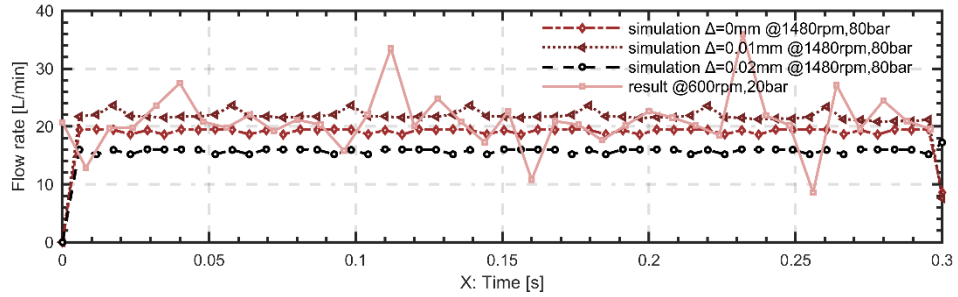

(b)

Fig. 6. Comparison of the simulated and experimental measured pressure and flow rate at 1480 rpm and 80 bar. Behavior of the outlet pressure oscillations (a) and outlet flow oscillations (b) are shown.

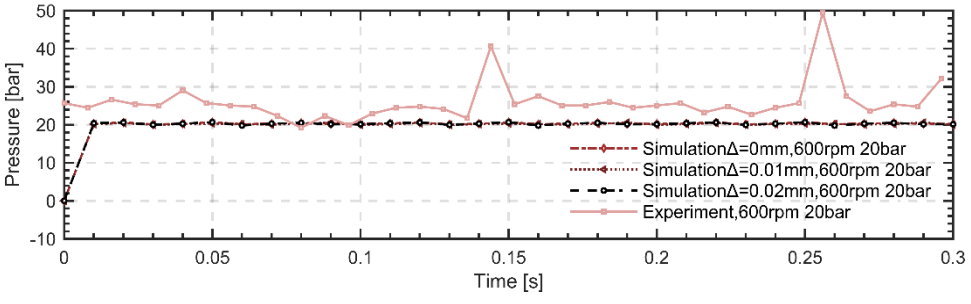

(a)

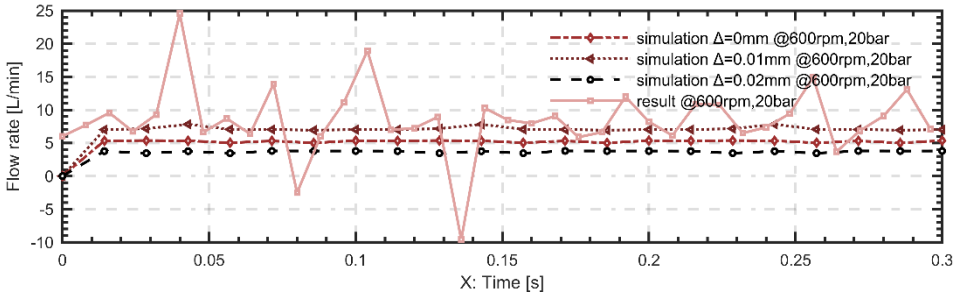

(b)

Fig. 7. Comparison of the simulated and experimental measured pressure and flow rate at 600 rpm and 20 bar. Behavior of the outlet pressure oscillations (a) and outlet flow oscillations (b) are shown.

6. Conclusions

This paper presents an experiment and numerical approach of modeling circular-arc gear pumps considering the center distance deviation. A review on the gear profiles design of circular-arc gear pumps was first provided, and the numerical modeling of circular-arc gear pumps then described. This numerical approach for modeling the geometric evolutions of the displacement chambers permitted to study the kinematic flow ripple of circular-arc gear pumps. The numerical model of an arc gear pump was established, in which the arc tooth profile can be accurately obtained, and the center distance deviation was considered in advance. In different center distances, the pressure ripple and flow ripple have been carried out in the light load condition and in the medium load condition with outlet pressures of 20, and 80 bar and the constant rotational speed of 600 rpm and 1480 rpm. The results show that with the increase of center distance deviation, the outlet flow rate of the arc gear pump increases first and then decreases greatly. The center distance deviation has little effect on the independent tooth cavity pressure. In the final section of the paper, the proposed fluid dynamic model is used to simulate a commercial circular-arc gear pump, which was tested within this research for modeling validation purposes. The simulated outlet pressure and outlet flow ripple are compared against the measured values. The comparisons highlight the validity of the proposed simulation approach. Next, the model can be used to gain further insights on the circular-arc gear pump operation, such as including localized cavitation, internal flow leakages. In order to give full play to the good transmission performance of the arc gear pump and prevent excessive

dynamic impact due to the center distance deviation, the dynamic response caused by the center distance deviation can be adjusted by optimizing the machining accuracy and assembly accuracy of the arc gear.

References

[1] Costa, G. K., & Sepehri, N. (2018). Understanding overall efficiency of hydrostatic pumps and motors. International Journal of Fluid Power, 19 (2), 106-116.
[2] Choudhury, S. K., Sa, P. K., Bakshi, S., & Majhi, B. (2016). An evaluation of background subtraction for object detection vis-a-vis mitigating challenging scenarios. IEEE Access, 4, 6133-6150.
[3] M.A. Morselli, La drastica evoluzione segnata dalle pompe a ''contatto continuo'': Part 1, Oleodinamica e Pneumatica, January 2005 (in Italian).
[4] Chen, C. O. K., & Yang, S. C. (2000). Geometric modelling for cylindrical and helical gear pumps with circular arc teeth. Proceedings of the Institution of Mechanical Engineers, Part C: Journal of Mechanical Engineering Science, 214(4), 599-607.
[5] Zhou, Y., Hao, S., & Hao, M. (2016). Design and performance analysis of a circular-arc gear pump operating at high pressure and high speed. Proceedings of the Institution of Mechanical Engineers, Part C: Journal of Mechanical Engineering Science, 230 (2), 189-205.
[6] Manring, N. D., & Kasaragadda, S. B. (2003). The theoretical flow ripple of an external gear pump. J. Dyn. Sys., Meas., Control , 125 (3), 396-404.
[7] Huang, K. J., & Lian, W. C. (2009). Kinematic flowrate characteristics of external spur gear pumps using an exact closed solution. Mechanism and Machine Theory, 44 (6), 1121-1131.
[8] Zhao, X., & Vacca, A. (2017). Formulation and optimization of involute spur gear in external gear pump. Mechanism and Machine Theory, 117, 114-132.
[9] Rundo, M. (2017). Models for flow rate simulation in gear pumps: A review. Energies, 10 (9), 1261.
[10] Rana, D., & Kumar, N. (2014). Experimental and computational fluid dynamic analysis of external gear pump. International Journal of Engineering Development and Research, 2 (2).
[11] Zhao, X., & Vacca, A. (2018). Analysis of continuous-contact helical gear pumps through numerical modeling and experimental validation. Mechanical Systems and Signal Processing, 109, 352-378.
[12]A. Vacca, M. Guidetti, Modelling and experimental validation of external spur gear machines for fluid power applications, Simul. Model. Pract. Theory19 (9) (2011) 2007–2031.
[13]AMESim 4.2 User Manuel. <http://nupet.daelt.ct.utfpr.edu.br/ontomos/paginas/AMESim4.2.0/doc/pdf/manuals/amesim.pdf>.

Declaration

List of abbreviations

N	the number of teeth
θ_A	the angle $\angle MO_1A$
θ_C	the angle $\angle MO_1C'$
θ_B	the angle $\angle MO_1B'$
r	the radius of the base circle
r_1	the radius of the base circle of driving gear
r_2	the radius of the base circle of driven gear
r_a	the addendum radius of gear
r_f	the root radius of gear
α	the angle $\angle Q'O_1M$
φ_1	a parameter related to the arc angle of the AB segment
φ_2	a parameter of the arc angle of the CD segment
ΔL	center distance deviation
β	the spiral angle

K	the bulk modulus
V	the instantaneous tooth space volume
$\dot{V}$	the change rate of tooth space volume
Q	the flow in the tooth space
h	the height of the leakage gap
L	the length of the leakage gap
b	the width of the leakage gap
u_s	the shearing velocity of the wall along the flow direction

Ethics approval and consent to participate

Not applicable.

Consent for publication

Not applicable.

Availability of data and materials

The datasets used and/or analysed during the current study are available from the corresponding author on reasonable request.

Competing interests

The authors declare that they have no competing interests

Funding

The authors received no financial support for the research, authorship, and/or publication of this article.

Authors' contributions

Xiaoling WEI has provided the design of the work, and has acquired and analyzed the data. Yongbao FENG has substantively revised it. Zhenxin HE has interpreted the data. Ke LIU has used the software to achieve the goal in the work.

Acknowledgements

This work has been developed in the Shandong Shijing Machinery Co., Ltd. The authors wish to thank Qingwu MENG and Guangzhi ZHANG for providing the experimental equipment and technical support.

Authors' information

W is a PhD candidate at Rocket Force University of Engineering. She has engaged in intelligent hydraulic components design and hydraulic system analysis for 8 years.

F is a doctor. He is currently a professor at Rocket Force University of Engineering. His research interests include the equipment launch technology, hydraulic technology and other related fields.

H is a doctor. He is a lecturer at Rocket Force University of Engineering. His research interests include modeling, simulation and control of electro-hydraulic systems, and lifting robot technology.

L is a postgraduate at Rocket Force University of Engineering. His research interests include intelligent hydraulic components design.